CHAPTER 2

SELECTION EFFECTS

2.1 INTRODUCTION

We begin this thesis with a study of the instrumental limitations of pulsar surveys, with particular reference to the IIMS. To quote a few examples of these limitations, the sky coverage of a pulsar survey is mainly limited by the geographical location of the radio telescope; its collecting area coupled with the sophistication of the electronics and the background sky temperature determines its sensitivity to weak pulsars; etc. In specifying these limitations one commonly quotes the minimum detectable flux S_{min} that a pulsar must posses (given its period, dispersion measure, luminosity, position in the sky, etc.) to be detected by the survey* It is currently believed that a satisfactory representation of S_{min} is given by (Taylor and Manchester 1977)

$$S_{min} = S_0 \beta (1 + T_{sky}/T_R)(1 + DM/DM_0)^{1/2} \qquad (2.1)$$

where T_{sky} and T_R are the sky and receiver noise temperatures, DM is the dispersion measure, D is a constant, S_0 is the minimum sensitivity of the survey and β is a factor (greater than 1) representing the reduction in sensitivity resulting from displacement of the source from the beam centre* In eq. (2.1), S_{min} does not dependupon the period P of the pulsar* Indeed, Taylor and Manchester (1977) only refer to a limiting period (of the order of tens of milliseconds) above which the sensitivity of the survey is believed to be uniform, and below which the sensitivity decreases rapidly. However, Huguenin (1976) has pointed out that short-period, high-dispersion pulsars are very difficult to observe. Much earlier, Large and Vaughan (1971) had demonstrated the presence of a selection effect, dependent both on P and DM , in the First Molonglo Survey (IMS). Because the IMS used a different method for pulsar search than that currently employed, their results are not directly relevant today.

In this chapter we argue that two modifications to eq. (2.1) are necessary* First, S_{min} depends not on the dispersion measure DM alone, but on DM/p (this is related to the effect discussed by Large and Vaughan (1971)). Hence short period pulsars are more difficult to detect than eq. (2.1) would suggest* Secondly, high declination δ pulsars are somewhat easier to detect because the IIMS spends longer observing times at higher declinations. Equation (2.6) gives a new formula for S_{min} incorporating these new effects.

Table 2.1 shows that the above effects are indeed present in the IIMS. Table 2.1(a) considers the IIMS pulsars in three period bins* In each bin we have tabulated (i) the number of pulsars (n_0) detected below the quoted minimum detectable flux, i.e., pulsars with $S_{PSR}/S_{min} < 1$ where S_{min} is given by eq. (2.1), (ii) the total number of pulsars detected n_0+m_0,

TABLE 2.1

Each column shows (i) observed number of pulsars (n_o) with S_{PSR} / $S_{min} < 1.0$, (ii) all pulsars in that bin ($n_o + m_o$), (iii) expected number (n_e) with $S < S_{min}$ in the bin, (iv) the difference ($n_o - n_e$), and (v) standard deviation (σ) on $n_o - n_e$.

(a) Pulsars in bins of period (in seconds). S_{min} was derived using eq. (2.1).

	$0.0 \leq P < 0.5$	$0.5 \leq P < 1.0$	$1.0 \leq P < 1.5$
n_o	11	21	19
$n_o + m_o$	76	89	40
n_e	18.9	22.1	10.0
$n_o - n_e$	-7.9	-1.1	9.0
σ	3.0	2.9	2.5

(b) pulsars in bins of declination. S_{min} was derived using eq. (2.1)

	$0^\circ \leq dec < 30^\circ$	$30^\circ \leq dec < 60^\circ$	$60^\circ \leq dec < 90^\circ$
n_o	18	26	16
$n_o + m_o$	97	89	38
n_e	26	23.8	10.2
$n_o - n_e$	-8.0	2.2	5.8
σ	3.3	3.2	2.5

(iii) the expected number of pulsars n_e with $S_{PSR}/S_{min}<1$, based on the total number n_0 in all bins, $n_e=(n_0+m_0)(\Sigma n_0)/\Sigma(n_0+m_0)$, expected on the null hypothesis that S_{min} is independent of P and δ, (iv) the difference n_0-n_e, and (v) the expected standard deviation σ on n_0-n_e. The values of σ quoted are not equal to the corresponding $(n_e)^{1/2}$ but have been computed including the fluctuations and correlations of all variables in n_e. It is reasonable to expect that n_0 should differ from n_e by a quantity of the order of σ. Table 2.1(a) shows that this is clearly not so. We obtain a ^{2} (computed as $\Sigma\left[(n_0-n_e)^2/\sigma^2\right]$) of 20.6 against the expected value of 3.0 implying that S_{min} probably has some ?-dependence in addition to the factors written down in eq. (2.1). In table 2.1(b), which considers the declination dependence, we similarly obtain a χ^2 of 11.8 against 3.0. These results appear to suggest that eq. (2.1) may not be an adequate description of the selection effects in pulsar surveys.

2.2 THEORY OF SELECTION EFFECTS

In fig. 2.1 we have schematically plotted the signal as a function of time in the de-dispersed folded output from a pulsar survey* The plot is for a duration of one period, and the signal strength is measured in units of temperature* Due to the ionized interstellar medium, the intrinsic pulse width W is broadened to $W+t$, where t is the dispersion broadening in a single frequency channel, In what follows, we assume that (i) the signal is folded at the correct P of the pulsar, (ii) the time resolution of the data is $1/\Delta\nu$ where $\Delta\nu$ is the bandwidth,

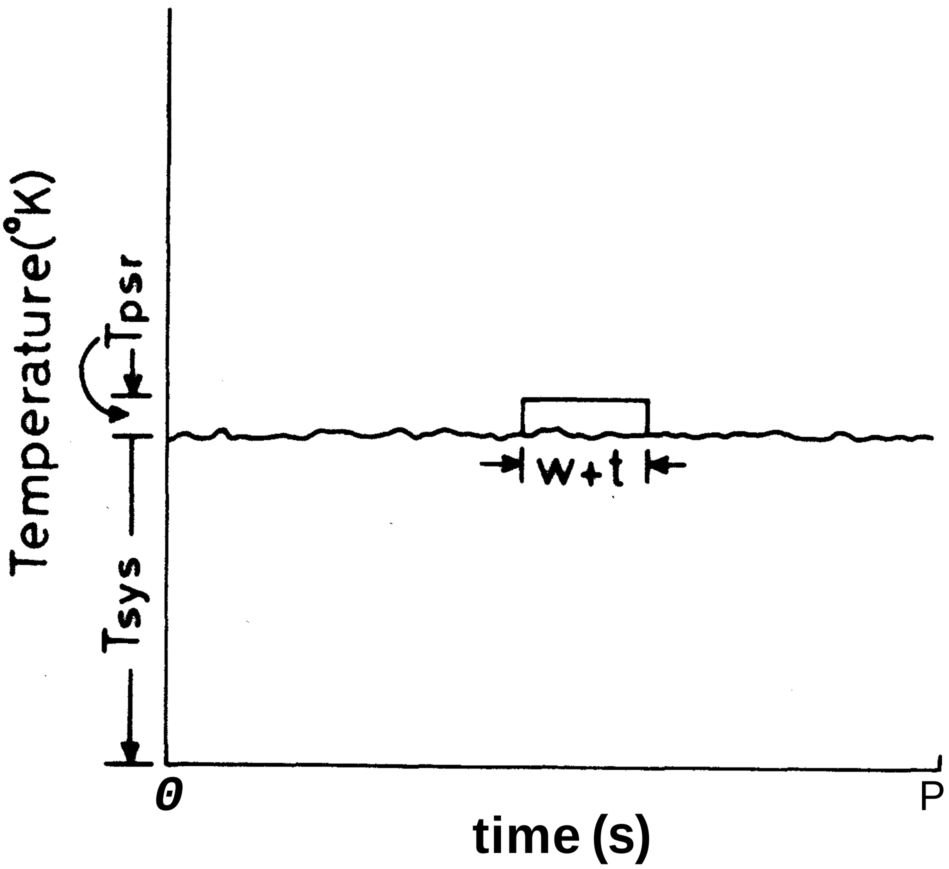

FIG.2.1 A schematic folded output from a pulsar survey. T_{sys} is the system noise level, and T_{PSR} is the mean pulsar level for the pulse duration. The pulse of intrinsic width w is broadened by t because of dispersion in the interstellar medium. For convenience in presentation the fluctuations in T_{sys} have been scaled down.

(iii) the signals in the various channels have been de-dispersed with the correct delay, and (iv) the position of the pulse and its width $W+t$ have been properly identified in the folded output* We later show that (ii) is not a necessary requirement.

Let the mean system temperature without the pulsar be T_{sys} . This is the receiver temperature T_R plus the background sky contribution; so

$$T_{sys} = T_R\,(1 + T_{sky}/T_R) \tag{2.2}$$

Let the pulsar under consideration, with mean signal strength T_{PSR} within the pulse window, be just at the threshold of detectability. For detection, the difference between the mean level $T_{PSR}+T_{sys}$ on-pulse and the mean level T_{sys} off-pulse should be some factor n (typically 5) times the noise σ_{diff} on the difference* Now

$$\begin{aligned}\sigma_{diff} &= \left[\sigma_{on}^2 + \sigma_{off}^2\right]^{1/2} \\ &= \left[\frac{T_{sys}^2}{(\tau/P)(W+t)\Delta\nu} + \frac{T_{sys}^2}{(\tau/P)(P-W-t)\Delta\nu}\right]\end{aligned} \tag{2.3}$$

where τ is the total observation time per sky position. Hence at the threshold of detection

$$T_{PSR} = \frac{n\,T_R}{(\tau\Delta\nu)^{1/2}}\left(1+T_{sky}/T_R\right)\left(\frac{P}{W+t}\right)^{1/2}\left(1+\frac{W+t}{P-W-t}\right)^{1/2} \tag{2.4}$$

T_{PSR} can be written in terms of the mean pulsar flux density S_{PSR} (energy per pulse divided by the period) as

$$T_{PSR} = \frac{1}{\beta}\,S_{PSR}\left(\frac{P}{W+t}\right)\frac{A}{k_B} \tag{2.5}$$

where β has been defined in eq. (2.1), A is the effective collecting area of the telescope and k_B is the Boltzmann's constant, Let us use the symbol d for the pulsar duty cycle (W/P), and write the dispersion broadening explicitly as $t = K_1 DM$ where K_1 is a constant proportional to $\Delta\nu$. Further, the total observational time $\tau = \tau_0/\cos\delta$ for transit observations such as IIMS where τ_0 is assumed to be a constant for a given survey* We then obtain

$$S_{min} = \beta S_0 (1 + T_{sky}/T_R)(d/d_0)^{1/2}\left[1 + \frac{K_1 DM}{Pd}\right]^{1/2}\left[1 + \frac{Pd + K_1 DM}{P - Pd - K_1 DM}\right]^{1/2}(\cos\delta)^{1/2} \quad (2.6)$$

where d_0 is a reference value of the duty cycle for all pulsars (taken to be 0.04) and S_0 is defined by

$$S_0 = n T_R k_B d_0^{1/2} / \left[A(\tau_0 \Delta\nu)^{1/2}\right] \quad (2.7)$$

which is a constant for a given survey (assuming A is independent of δ as is true for the IIMS). For convenience, we will refer to the term $(d/d_0)^{1/2}$ as term A, the terms in the first and second square brackets in eq. (2.6) as terms B and C respectively, and the term $(\cos\delta)^{1/2}$ as term D. In eq. (2.6) the term C is not prominent until the pulse width $W+t$ becomes a significant fraction of P. Since, this is rare, except when the effects of multipath propogation become overwhelming, C can usually be taken as 1. The term D essentially represents the increased integration time at higher declinations for surveys such as the IIMS, The term B has a non trivial P dependence which we wish to highlight in this chapter* In the light of this term, we see that eq. (2.1) is valid only at one value of the period, P_0, which can be obtained by equating $P_0 d_0/K_1$ in eq. (2.6) to DM_0 in eq, (2.1). If P_0 turns out to be the

This term would be absent for the Jodrell Bank survey which tracked the search regions, and would be more complicated for the Arecibo survey average period (~ 0.7 s.) for pulsars, one might argue that eq. (2.1) is valid in an average sense. However, the values of P_0 which we obtain for the three major surveys, viz., the Jodrell Eank survey, the Arecibo survey and the IIMS (referred to in chapter 1), are 3.0, 0.8 and 1.6 seconds respectively* We thus conclude that eq. (2.1) does not properly represent the selection effects at low periods, where significant fractions of the Galaxy might be relatively inaccessible to the surveys. As an illustration, for $P < 0.4$ s., the sensitivity of the IIMS is reduced by more than $\sqrt{2}$ over more than 90% of the volume of the Galaxy. The term A in eq. (2.6) shows the variation of S_{min} with duty cycle d . This term is important if $t < w$, when the term B collapses to ~ 1. If $t \gg w$, the $d^{1/2}$ in A is approximately cancelled by $d^{-1/2}$ in B.

What happens when the pulse width $w+t$ is not resolved in the integrated profile? This occurs for nearly 20% of the pulsars detected by the IIMS where the minimum time resolution was not $1/\Delta\nu$ but a much smaller quantity t_0 =20 ms. In the case when $w+t < t_0$, $w+t$ is to be replaced by t_0 in both eq (2.4) as well as eq (2.5). Consequently eq (2.6) will imply that $S_{min} \propto P^{-\frac{1}{2}}$. In the intermediate situation when w and t are both $< t_0$ but $w+t > t_0$, eq (2.6) continues to be valid. Thus in all cases, the period dependence of S_{min} remains and can not be neglected*

We should mention here that Large and Vaughan (1971) experimentally demonstrated the variation of S_{min} with both P and DM for the IMS. We have verified that their S_{min} (fig. 4 in their paper) depends approximately upon the specific combination DM/p as in our formula (term B). To make a more detailed comparison with our theory, we have estimated the function $V = -d(\log S_{min})/d(\log P)$ from their published curves of S_{min} for the three systems they have studied, viz., single channel, double channel and the 20 channel systems (figures 4, 5 and 6 respectively in their paper). In all cases we find that their results imply values of V greater than 0.5. On the other hand, our formula (eq (2.6)) shows that V should asymptotically tend to a maximum value of 0.5 at small periods (assuming that P is not so small that term C becomes important)+ It thus appears that the IMS had a stronger dependence of S_{min} on DM/p than we expect from our theory,

The discrepency between the results of Large and Vaughan and our theory is puzzling, since both refer to the same effect. We feel that it probably arises from the visual search method used in the INS to detect pulsars from the chart records* Considering the complex pattern recognition powers of the human eye it is quite possible that sensitivity falls off rapidly as pulses are broadened, Our formula, on the other hand, refers to a computer search on digitised data, which could have totally different sensitiviy characteristics.

2.3 EVIDENCE FROM PULSAR DATA

We have carried out some simple tests on pulsar observational data to confirm that the new selection effects discussed in the previous section really exist. The calculaions have been done on the sample of pulsars detected by the IIMS.

This is the most recent as well as the most extensive of all surveys, and yielded a total of 224 pulsars* In what follows, we assume that all pulsars have the same duty cycle d for the following reasons. Firstly, we feel that duty cycles which are derived from pulse equivalent widths W_e may not be appropriate in eq. (2.6). Some calculations we have done using eq. (2.6) do indeed suggest that W_e is an unreliable parameter for our purposes here. Secondly, d is found to be almost independent of P ; so this approximation will not introduce any systematic period-dependent effects into our results* Thirdly, the discussion in the previous section shows that the d -dependence in eq. (2.6) in likely to be weak in the majority of the cases* We therefore replace d by d_o in eq. (2.6) to obtain

$$S_{min} = \beta S_o \left(1 + T_{sky}/T_R\right)\left(1 + k_2 DM/p\right)^{1/2} (\cos \delta)^{1/2} \qquad (2.8)$$

where $k_2 = K_1/d_o$ is a constant,

Figures 2.2 and 2.3 show the results of some tests we have carried out on the IIMS data using the old (eq. (2.1)) and the new (eq. (2.8)) formulae for the selection effects* In fig. 2.2(a) we have plotted the number of pulsars detected (N_o) against a normalised flux χ (derived from eq. (2.1)).

$$\chi = S/\left[\beta (1 + T_{sky}/T_R)(1 + DM/DM_o)^{1/2}\right] . \qquad (2.9)$$

The pulsars have been sorted into bins of width 0.2 in $\log_{10} \chi$. Figure 2.3(a) shows the results using a similar definition of based on eq. (2.8). In both the figs. 2.2(a) and 2.3(a) N_o decreases at high χ because the pulsar number density itself decreases at high luminosities* N_o also decreases for

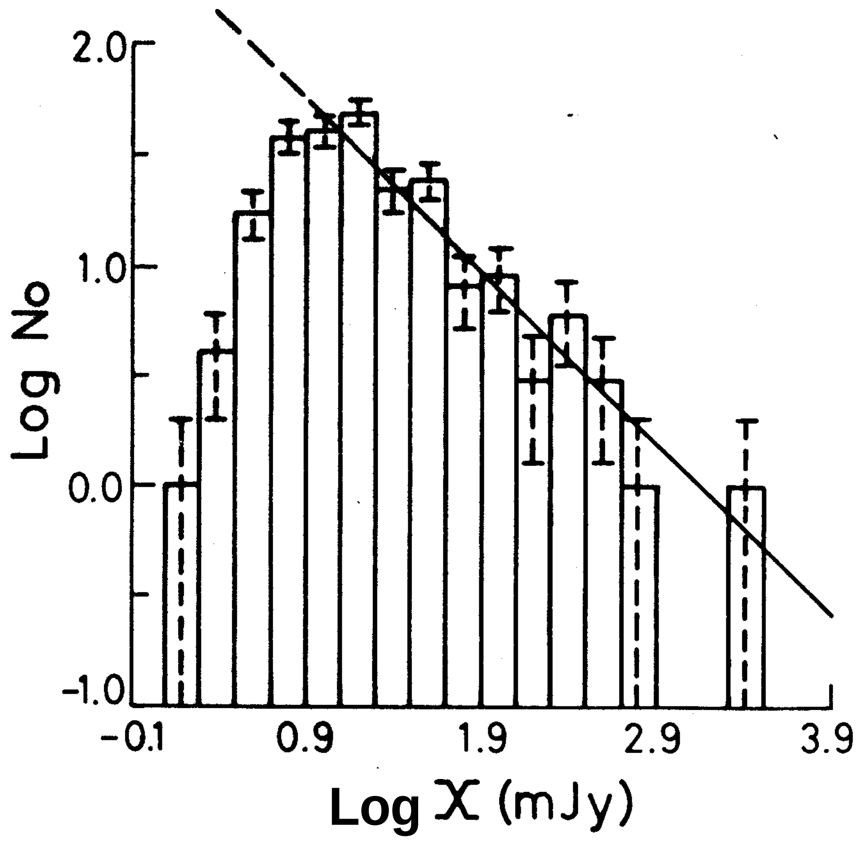

FIG. 2.2(a) Histogram of observed number of pulsars (N_o) against normalized **flux**
$X = S/\{\beta(1+T_{sky}/T_r)\ (1+D/D_o)^{\frac{1}{2}}\}$.
The error bars represent variance at the level of one standard deviation ($=(N_o)^{\frac{1}{2}}$). The solid line is the least squares fit of a straight line to the data in the descending limb of the histogram and gives the expected number of pulsars (N_e). The dashed line is its extrapolation.

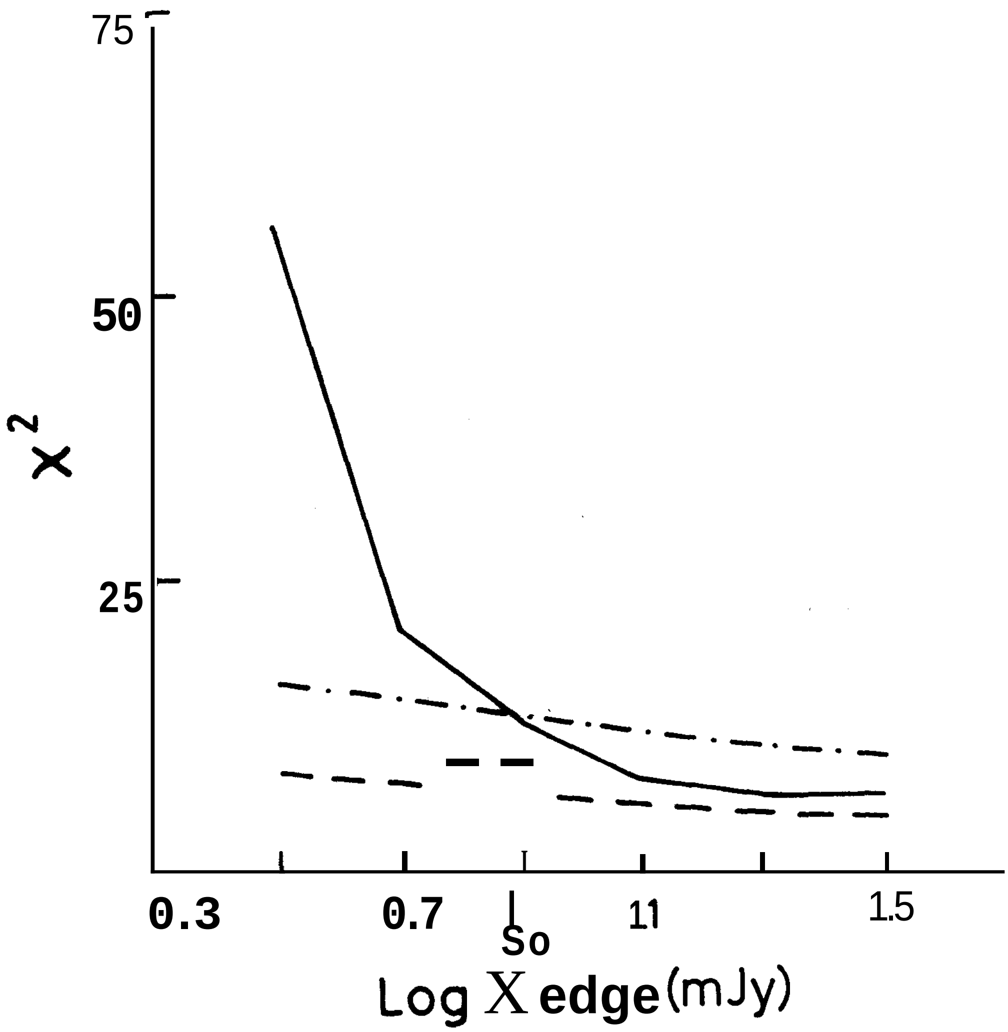

FIG. 2.2(b) Plot of χ^2 obtained by fitting the curve $N_e = \alpha X^{-\beta}$ to the descending limb in Fig. 2.2(a) (solid line), along with the expected value (dashed line) and its 95% confidence upper bound (chained line). X_{edge} is the lowest X value used in the curve fitting. The χ^2 increases rather abruptly from its normal value around $X_{edge} = S_o$, showing that the curve fitting has broken down.

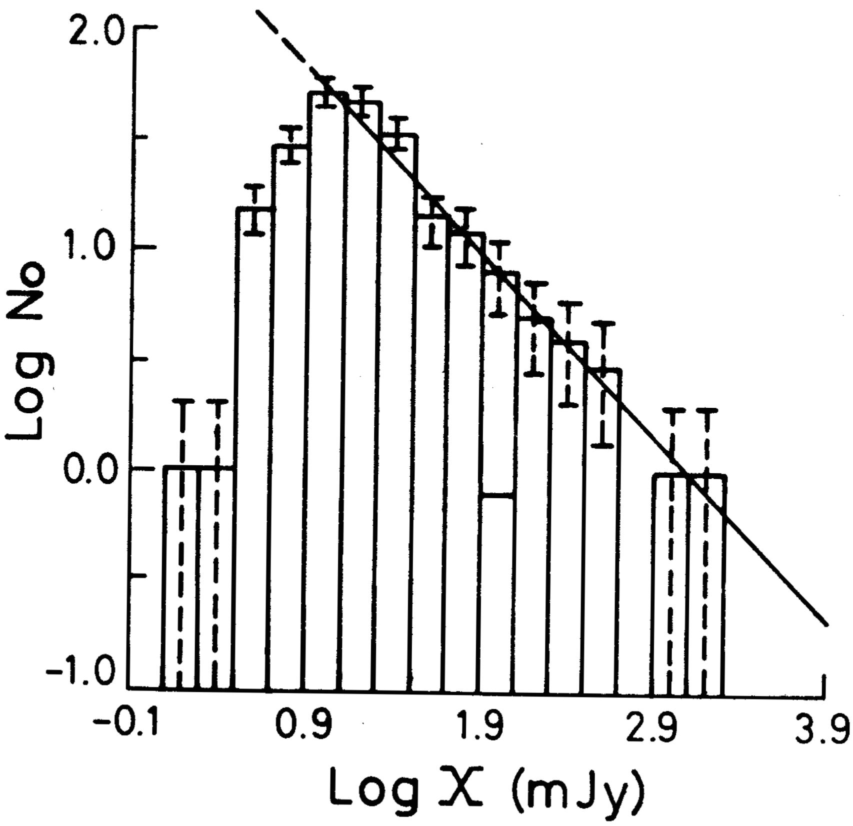

FIG. 2.3(a) Same as in Fig. 2.2(a), with
$X = S / \{ \beta (1 + T_{sky}/T_r)(1 + K_2 D/P)^{\frac{1}{2}} (\cos(\delta))^{\frac{1}{2}} \}$

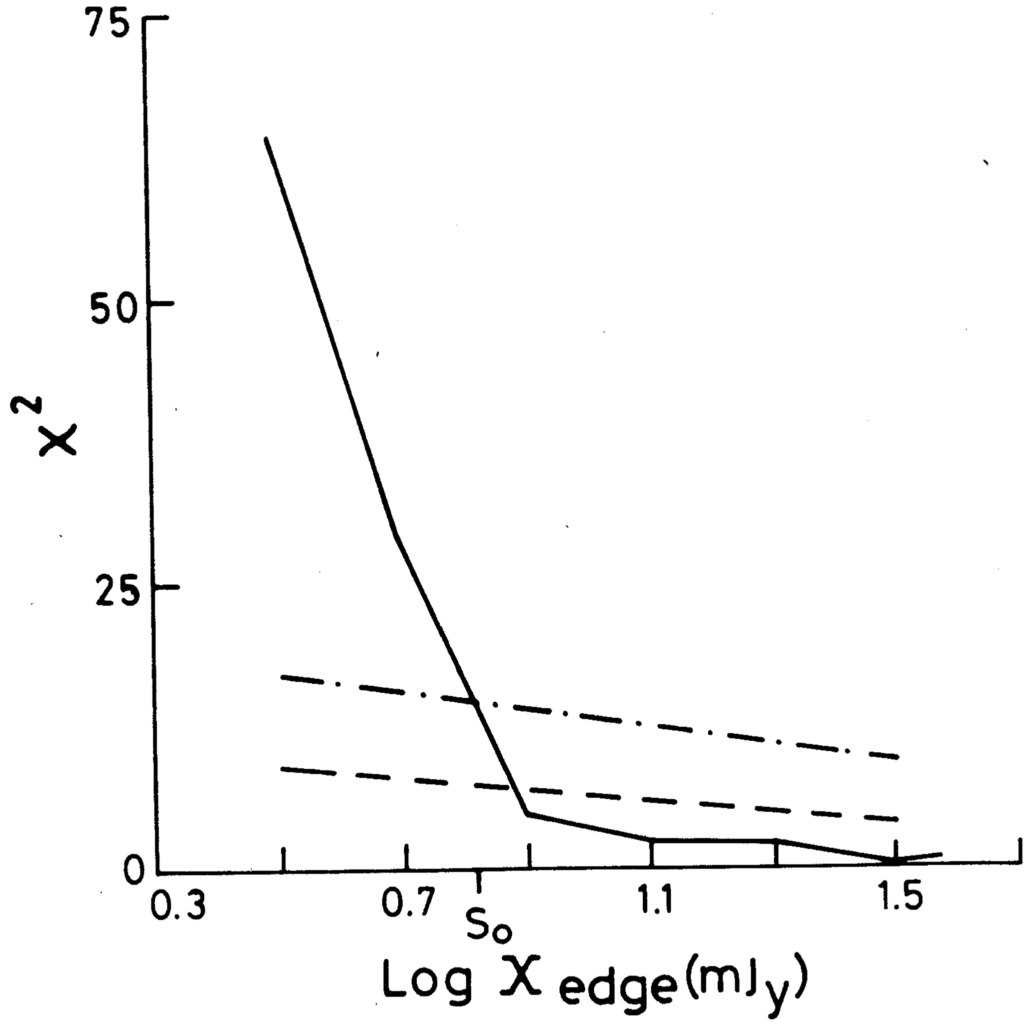

FIG. 2.3(b) Same as in Fig. 2.2(b), with

$$X = S/\{\beta(1+T_{sky}/T_r)\ (1+K_2D/P)^{\frac{1}{2}}\ (\cos(\delta))^{\frac{1}{2}}\}$$

low values of X (below S_o) because of the reduced sensitivity of the survey* Under ideal conditions, this transition should be quite sharp, around $X = S_o$. However, in actual practice it is broadened* Firstly there is a statistical broadening caused, among other things, by the variability of pulsar luminosities (Krishnamohan 1981). Secondly, any unaccounted selection effect would broaden the transition* The width of the transition region σ_{t+} can therefore be used to decide which of the equations (2.1) and (2.8) fits the IIMS data better.

Another test is the number of pulsars below $X = S_o$. As mentioned before, under ideal conditions the transition region is very sharp and there will be no pulsars below S_o. Any selection effect tends to smear out S_o so that there are now pulsars below it.

To carry out the above tests we had first to determine S_o for eq. (2.1) and eq. (2.8). This was done as follows+ Starting with fig. 2.2(a), we initially assumed a certain value of X on the descending limb of N_o vs. X to be S_o. We took all bins above this value of X (we shall call it X_{edge}) and fitted a curve of the form $N_e = \alpha X^{-\beta}$ (suggested by the data itself) by least squares* This curve gives the expected number of pulsars N_e at each X. We computed a χ^2 as

$$\chi^2 = \sum (N_o - N_e)^2 / N_e \qquad (2.10)$$

where the summation is over all bins above X_{edge}, and used it a measure of the goodness of the curve fit. We repeated this exercise for successively lower values of X_{edge} where the fit becomes progressively poorer since one begins to include data from the transition region also* In fig. 2.2(b) we have plotted χ^2 as a function of X_{edge} along with the expected χ^2 (which is the number of bins above X_{edge} minus two, for two parameters fitted) and the 95% upper bound on the expected χ^2. The observed χ^2 is normal at large X_{edge} and increases rapidly at small X_{edge} as expected. By interpolation, we obtained the value of X_{edge} where the observed χ^2 just equals the 95% confidence upper bound. At this value of X_{edge} the curve fitting is seen to definitely break down. We adopted this value of X_{edge} as S_0 Although this approach tends to underestimate S_0, it has the important merit of being an objective way of analysing the data. We obtain S_0 =7.6 mJy, or βS_0 =7.9mJy, which is close to the quoted value of 8.0 mJy. We interpret this agreement as lending support to the validity of our approach. A similar exercise with fig. 2.3(a) gives S_0 =6.6 mJy.

We then computed the width of the transition region(σ_{t+}) in fig* 2.2(a) using the estimate

$$\sigma_{t+}^2 = \Sigma\, \omega_i (\log x_i - \log S_0)^2 / \Sigma\, \omega_i \tag{2.11}$$

where $\omega_i = N_0/N_e$ is the weight in each bin. The summation in eq. (2.11) is taken over all bins below S_0 We obtain σ_{t+} =0.20. For.fig. 2.3(a) we get σ_{t+} =0.15. Comparing the results of fiures 2.2 and 2.3 we see that (1) the width of the transition is reduced by incorporating the period and declination dependent selection effects through eq. (2.8), and (2) there are 60 pulsars below S_0 in fig. 2.2(a) and only 33 pulsars in fig* 2.3(a). Both these results support our

TABLE 2.2

Each column shows (i) observed number of pulsars (n_o) with $S_{PSR} / S_{min} < 1.0$, (ii) all pulsars in that bin ($n_o + m_o$), (iii) expected number (n_e) with $S < S_{min}$ in the bin, (iv) the difference ($n_o - n_e$), and (v) standard deviation (σ) on $n_o - n_e$.

(a) Pulsars in bins of period (in seconds). S_{min} was derived using eq. (2.8).

	$0.0 \le P < 0.5$	$0.5 \le P < 1.0$	$1.0 \le P < 1.5$
n_o	6	15	5
n_o+m_o	76	89	40
n_e	9.6	11.3	5.1
n_o-n_e	-3.6	3.7	-0.1
σ	2.3	2.4	1.9

(b) pulsars in bins of declination* S_{min} was derived using eq. (2.8)

	$0^\circ \le dec < 30^\circ$	$30^\circ \le dec < 60^\circ$	$60^\circ \le dec < 90^\circ$
n_o	15	11	7
n_o+m_o	97	89	38
n_e	14.3	13.1	5.6
n_o-n_e	0.7	-2.1	1.4
σ	2.6	2.6	2.0

contention that eq. (2.8) is a better representation of the selection effects in the IIMS than eq. (2.1).

Finally we have repeated the calculations of table 2.1 using eq. (2.8) with S_0 =6.6 mJy, instead of using eq. (2.1) with S_0 =8.0 mJy. The results are shown in table 2.2. We have computed. a χ^2 similar to that we computed for table 2.1. We now obtain a χ^2 of 5.0 in table 2.2(a) and a χ^2 of 1.2 in table 2.2(b) as against the expected value of 3.0. In both cases there is a clear improvement over the results of table 2.1.

2.4 DISCUSSION

The various tests described above would appear to confirm the presence of period-dependent and declination-dependent selection effects in the IIMS. However, because of the noisy data, we believe the strongest argument is really the discussion of section 2.2 which says such effects must exist.

Throughout this chapter as well as in the next chapter, we have used the IIMS data which was first published in the preprint form (Manchester et. al. 1978). This data differs slightly from the corresponding data published in the latest pulsar catalogue by Manchester and Taylor (1981). The major difference occurs in the pulsar radio fluxes (at 408 MHz), albeit in a few pulsars only, mainly because pulsars are intrinsically variable creatures. We have ascertained that these changes in the basic pulsar data do not alter any of our conclusions. Some of the calculations in the chapters to come have been done on both the sets of data and they do not differ siqnificantly.

CHAPTER 3

INTERSTELLAR ELECTRON DENSITY

3.1 INTRODUCTION

The interstellar electron density n_e is an important parameter in pulsar studies since it is used to determine pulsar distances d (pc) from their observed dispersion measure DM (pc cm^{-3}). Hall (1980) has summarised in detail the various previous attempts to estimate n_e. The most reliable studies have used the DM of the few pulsars for which independent distances have been measured through 21 cm. HI absorption measurements. However, the mean electron density $\langle n_e \rangle$ thus obtained is not precise enough; further independent studies are necessary to determine it accurately. To our knowledge the only other independent study is that by del Romero and Gomez-Gonzalez (19811, based on the a priori assumption that pulsars are predominantly a spiral arm population* In this chapter we discuss yet another independent study of n_e under the assumption that the galactic pulsar population is azimuthally symmetric about the galactic centre.

3.2 METHOD OF ANALYSIS

All our calculations are based on the assumption of azimuthal symmetry for the galactic pulsar population. The Sun is taken to be situated 10 kpc from the galactic centre* We describe here the basic method employed to determine a uniform mean electron density $\langle n_e \rangle$ for the whole Galaxy. We then discuss the modifications made in order to study more complicated models of n_e .

It is clear that the observed pulsar distribution will be consistent with cylindrical symmetry about the galactic centre for only a limited range of values of $\langle n_e \rangle$. Distance estimates of pulsars obtained using the relation

$$\langle n_e \rangle = DM/d \tag{3.1}$$

with over-large values of $\langle n_e \rangle$ would appear to move the centre of gravity of the pulsar distribution away from the galactic centre towards the Sun (after allowing for selection effects), while the converse would be true for too small values of $\langle n_e \rangle$. In our calculations we assume a value of $\langle n_e \rangle$ and compute the corresponding positions of the observed pulsars in the Galaxy. For each pulsar we consider a circle passing through it, centred on the galactic centre and parallel to the galactic plane (fig. 3.1 shows the circle projected on to the plane of the Galaxy). We then compute X_{obs} , the projection of the derived radius vector from the galactic centre to the pulsar on to the line joining the Sun and the galactic centre* We also compute X_{exp} , the expected value of X for the circle, considering all seletion effects and assuming a. uniform probability of pulsar occurrence around the circle* Since for a given pulsar period and luminosity only a portion of each circle is visible

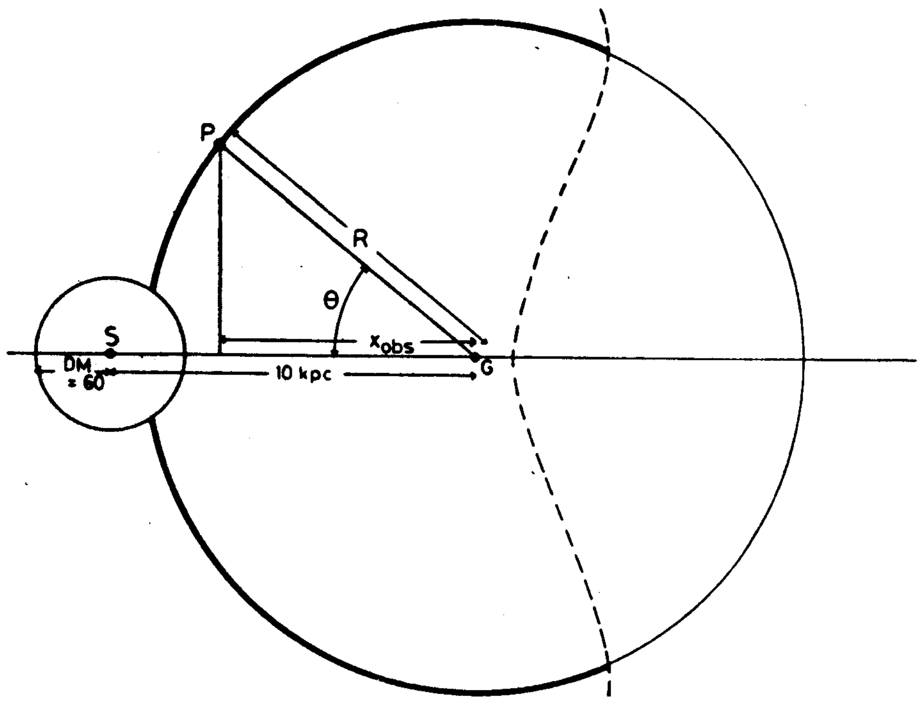

FIG. 3.1 Schematic illustration of a typical pulsar P and its corresponding galactocentric circle, both projected onto the galactic plane. G is the centre of the Galaxy. Around the Sun S an approximately spherical volume of radius corresponding to a dispersion measure of 60 pc. cm^{-3} is removed in our calculations for reasons discussed in the text. The dashed curve represents a typical viewing limit for the IIMS. For our calculations, we require (i) X_{obs}, the projection of the radius PG onto the line SG, (ii) X_{exp}, the mean value of the projection averaged over the visible portion of the pulsar circle (thick line), and (iii) a ^{2} , the variance of the projection, obtained by averaging the deviation $(X-X_{exp})^2$ over the visible portion of the circle. These quantities are obtained for each pulsar for a given model of the galactic electron density and used in eq. (3.2) to compute Y. Note that $|\theta|$ could have been used in place of X; however the sensitivity of the test is found to decrease.

to the pulsar surveys on Earth due to the various selection effects in pulsar searches (discussed in detail in chapter 2), X_{exp} is generally different from zero. Finally we compute the following mean deviation

$$Y(\langle n_e \rangle) = \sum_{i=1}^{N} \omega_i \left[X_{obs,i} - X_{exp,i} \right] / \sigma_i \qquad (3.2)$$

where σ_i is the calculated variance on $X_{obs,i}$. The summation is over all the pulsars included in our calculations and ω_i is a weight given to the contribution from the i^{th} pulsar* ω_i is estimated on the basis of the effective contribution of the pulsar to our test, which in turn depends upon its radio luminosity. Pulsars with high luminosity can be potentially detected far away from the Sun and are therefore best suited to test for a cylindrical distribution on a galactic scale, The lower luminosity pulsars are closer to the Sun, and so are of lesser importance to our calculations.We have investigated the sensitivity of our estimator $(X_{obs,i} - X_{exp,i})/\sigma_i$ to changes in $\langle n_e \rangle$ and have derived a simple weighting scheme in which pulsars with radio luminosity (at 400 MHz and assuming $\langle n_e \rangle = 0.03$ cm^{-3}) greater than 10 mJy Kpc are each given a weight of 1.5, those with luminosity less than 10 mJy Kpc but grater than 4 mJy Kpc are each given a weight of 1.0 and pulsars with still lower luminosities are eliminated altogether* These last pulsars are very close to the Sun and only add "noise" to the estimate of $Y(\langle n_e \rangle)$ in eq. (3.2). The particular choice of the projected distance X in eq. (3.2) was used in our calulations as it was found to be more sensitive than other choices such as $|\theta|$.

Since for the best value of $\langle n_e \rangle$, each of the terms

$(X_{obs,i} - X_{exp,i})/\sigma_i$ in eq. (3.2) has an expected mean of 0 and a standard deviation of 1, the mean value of Y is 0 while its variance σ_Y is given by

$$\sigma_Y^2 = \sum_{i=1}^{N} \omega_i^2 \qquad (3.3)$$

In our calculations, we therefore accept those values of $\langle n_e \rangle$ which lead to $(Y/\sigma_Y)^2 \leq 1$ and reject the rest.

The above procedure needs to be modified when testing more complicated electron density models, For example, in testing a model having the form

$$n_e(z) = n_e(0)\ \mathrm{EXP}-(|z|/z_0) \qquad (3.4)$$

we need to determine two parameters, $n_e(0)$ and z_0. We do this by testing the cylindrical symmetry of the pulsar distribution separately in the low-2 and high-z regions of the Galaxy, We choose to divide the pulsars into two classes such that the dividing value of $|z|$ represents the median $|z|$ for the sample* For each choice of $n_e(0)$ and z_0, we obtain Y_1, σ_{Y_1}, Y_2, σ_{Y_2} for the two regions separately. The criterion for the acceptability of the model is that

$$\xi = \left[(Y_1/\sigma_{Y_1})^2 + (Y_2/\sigma_{Y_2})^2 \right] \leq 1 \qquad (3.5)$$

We restrict our test to the 224 pulsars detected by IIMS since it is the most extensive survey and its selection effects are well understood. We have taken the minimum sensitivity S_0 to be 8.0 mJy and used eq. (2.8) of the previous chapter. We have employed three criteria to select a subsampie of the IIMS pulsars* Firstly, all low luminosity pulsars

(< 4 mJy Kpc^2) are given weights $\omega_i = 0$ as discussed earlier. Secondly, nearby pulsars are unreliable for our purposes since the dispersion measure contribution from HII regions canhave large fluctuations; this effect is expected to be less significant for most distant pulsars, Consequently, we have removed all pulsars with $DM < 60$ pc cm^{-3}, To be consistent, while computing $X_{exp,i}$ and σ_i , we deleted the appropriate segments of these circles which intersect this volume+ Thirdly, we have deleted all pulsars whose mean flux densities are below the detection threshold of the IIMS. This is necessary since we compute $X_{exp,i}$ on the basis of the assumed detection threshold, After this selection process we were finally left with a working sample of 52 pulsars, Figure 3.2 shows the distribution of these 52 pulsars projected on the galactic plane, The distances have been computed using the optimized electron density model of eq. (3.17). It should be noted that very few of these pulsars lie beyond the galactic centre, Therefore our tests may be expected to have rather limited sensitivity,

3.3 TESTS OF SOME SIMPLE MODELS

We have tested a number of simple electron density models that are currently popular,

3.3.1 UNIFORM ELECTRON DENSITY MODEL

Using the method described in section 3.2, we estimate the effective mean electron density in the Galaxy to be $\langle n_e \rangle = 0.037^{+0.02}_{-0.01}$ cm^{-3}, where the quoted errors represent

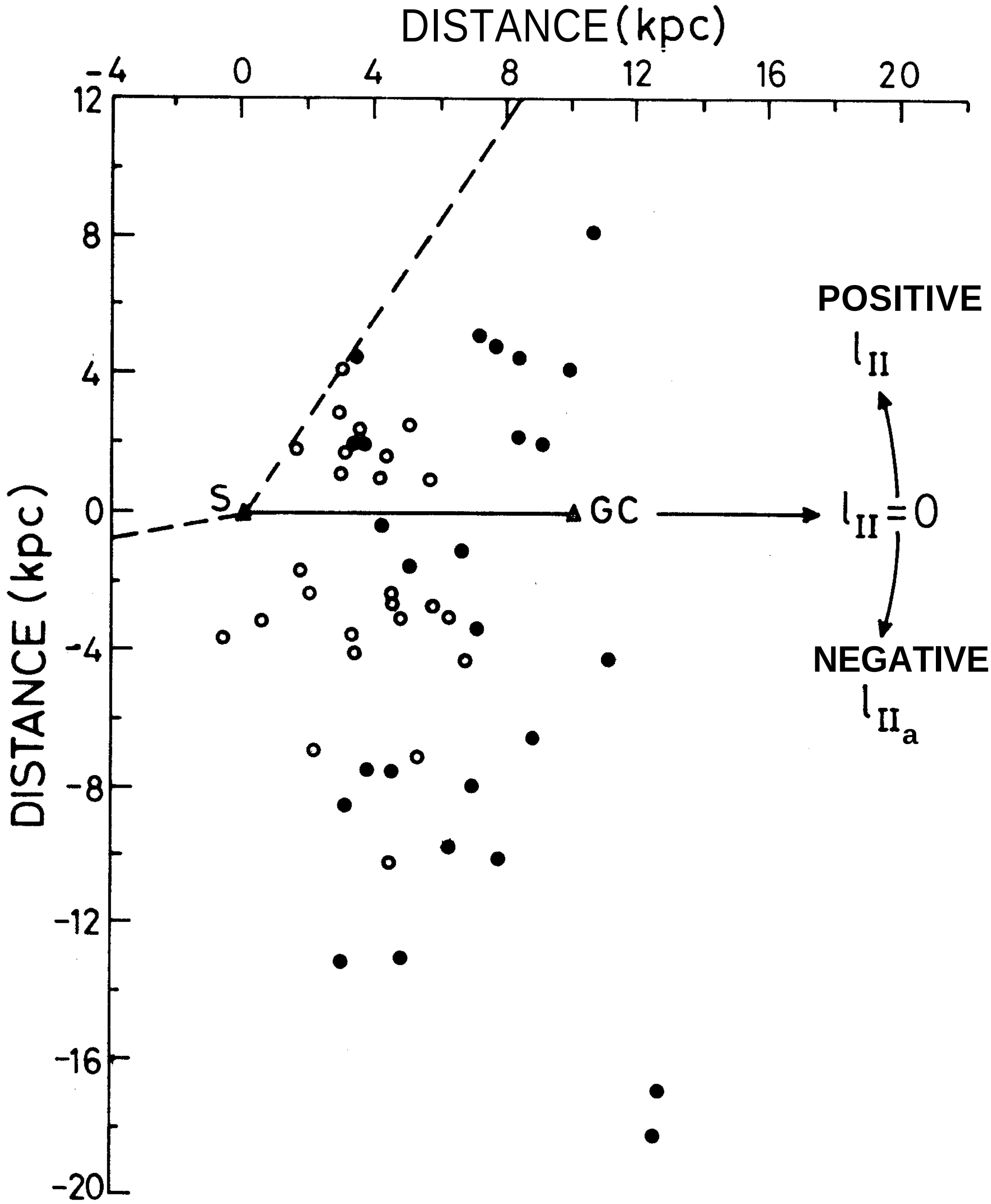

FIG. 3.2 Position of the 52 pulsars used in our calculations computed using eq. (3.17) and projected onto the galactic plane. The triangles S and GC mark the positions of the Sun and the Galactic Centre respectively. The dashed lines represent the longitude limits of the II Molonglo Survey in the galactic plane (corresponding to declination +20°). Filled circles represent more luminous pulsars which are given a higher weightage (weight = 1.5) in our calculations, as compared to the medium luminosity pulsars which are represented by open circles (weight = 1.0). Note that very few pulsars lie beyond the galactic centre, which might lead to a reduction in our sensitivity.

statistical fluctuations at the 1 σ level* Figure 3.3 shows the variation of Y/σ_Y as a function of the assumed $\langle n_e \rangle$ and illustrates our method of estimating the confidence limits on $\langle n_e \rangle$. Note that the lower bound is rather tight, suggesting that values below 0,025 cm^{-3} are unlikely, This is of interest because lower values of $\langle n_e \rangle$ have been commonly invoked to resolve the problem of high pulsar birthrates, We now find this improbable,

3.3.2 EXPONENTIAL MODEL

We have studied an exponential model of the form of eq. (3.4) by testing the pulsar distribution separately in high-z and low-z regions (boundary chosen to divide the pulsars equally in the two regions), as described in the previous section. We obtain bounds on $n_e(0)$ at each value of scale height z_0 based on the criterion of eq. (3.5). The results are shown as the two solid lines in fig, 3.4. For very low z_0 values ($<$ 250 pc), the eletron density decreases very rapidly with $|z|$, and it is impossible to account for the high DM of certain pulsars even by placing them at infinite distance from the Earth* The dashed line in fig. 3.4 is the locus of points at which about 20% of our 52 pulsars run into this problem. In our view, models lying below this line can definitely be rejected* Hall's model (1980), marked in fig. 3.4, is seen to lie outside this "allowed" region. The widely used model of Taylor and Manchester (1977) is aceptable.

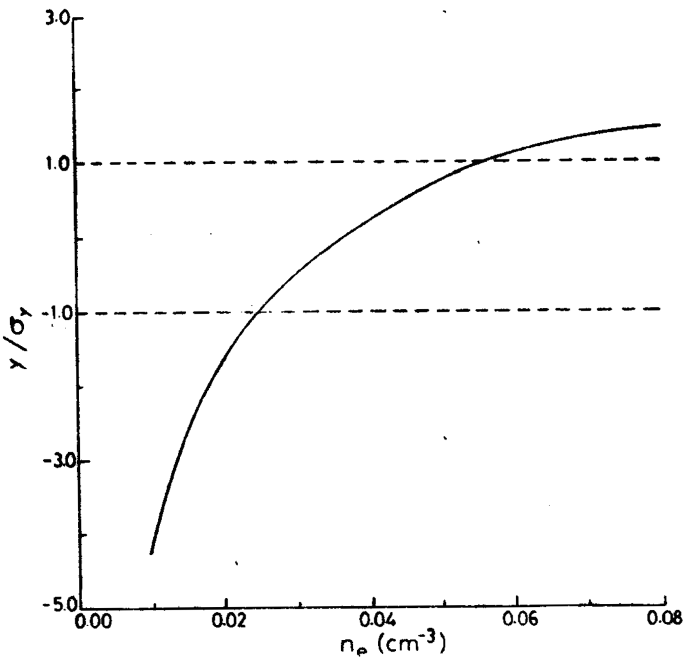

FIG. 3.3 Computed variation of Y/σ_Y as a function of the assumed $\langle n_e \rangle$. Allowed values of $\langle n_e \rangle$, for which $Y/\sigma_Y \leqslant 1.0$, lie within the dashed lines. The curve is very steep at low $\langle n_e \rangle$, allowing us to set confident lower limits on $\langle n_e \rangle$.

3.3.3 VATIATION OF ELECTRON DENSITY WITH GALACTIC RADIUS

We have studied an electron density model of the form

$$\langle n_e \rangle = n_{e<} , \quad R_{GC} < R_0$$
$$= n_{e>} , \quad R_{GC} > R_0 \qquad (3.6)$$

As before, we divide the Galaxy into two regions, an inner one ($R_{GC} < R'$) and an outer one $R_{GC} > R'$), where R'(Kpc) is chosen such that each region has approximately the same number of pulsars. We accept only those combinations of $n_{e<}$ and $n_{e>}$ for which eq. (3.5) is satisfied* Figure 3.5 shows the allowed combinations of $n_{e<}$ and $n_{e>}$ for R_0 =7 Kpc. There seems to be no reason to suspect significantly different values for $n_{e<}$ and $n_{e>}$, contrary to some recent suggestions, On the basis of fig. 3.4 and keeping in mind the evidence of earlier studies ' (Ables and Manchester 1976; del Romero and Gomez-Gonzalez 1951; Harding and Harding 1982) we suggest that $n_{e<}$ =0.04 cm^{-3} and $n_{e>}$ =0.03 cm^{-3} (R_0 =7 Kpc) may be a reasonable model* In fact, for pulsar studies, an $\langle n_e \rangle$ independent of R_{GC} is quite adequate. We note that the test is quite insensitive to the value of n_e in the very inner portion of the Galaxy (R_{GC} below, say, 5 Kpc) since very few of our pulsar lines of sight intersecct this region. We cannot therefore rule out a significantly higher $\langle n_e \rangle$ in this region.

314 CONTRIBUTION FROM HII REGIONS

So far we have neglected the effect of HII regions in our

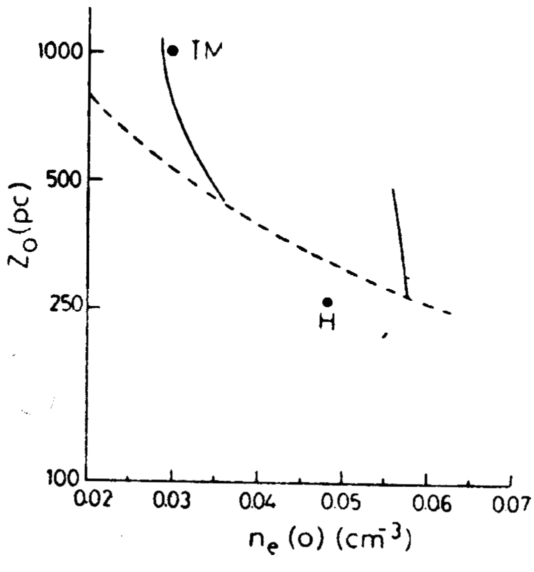

FIG. 3.4 Results for the exponential model of n_e (eq. (3.4)). The solid lines mark the lo limits of $n_e(0)$ at each z_o. The dashed line represents points at which the model is unable to explain the observed high dispersion measures of 11 of our 52 pulsars. Models corresponding to points below this line can definitely be rejected. The models proposed by Hall (1980) and Taylor and Manchester (1977) are marked by H and TM respectively.

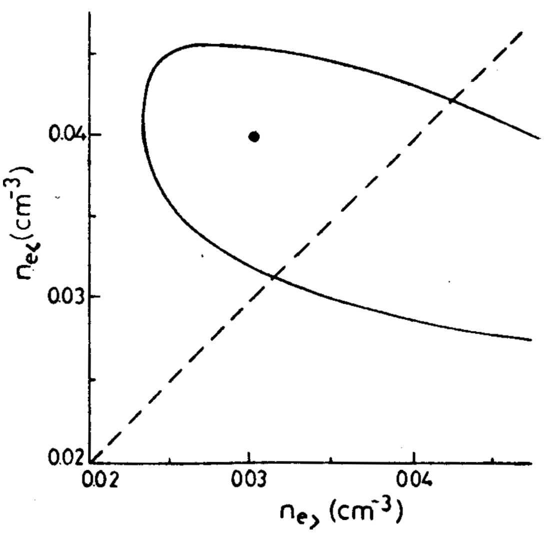

FIG. 3.5 Allowed combinations of $n_{e<}$ (in the inner regions of the Galaxy, R_{GC} < 7Kpc) and $n_{e>}$ (in the outer regions, R_{GC} > 7 Kpc) lie within the solid curve, which represents the la limits on these parameters. The allowed region is nearly equally distributed on either side of the $n_{e<} = n_{e>}$ line (dashed line in the figure). Therefore a uniform electron density model for the whole Galaxy is quite adequate. If at all, $n_{e>}$ appears to be larger than $n_{e<}$. However, since other studies seem to show that $n_{e<} > n_{e>}$, we suggest the model corresponding to the dot may be cfose to the truth.

calculations. HII regions are small volumes of (comparatively) extremely high electron densities, surrounding bright stars. It is quite common for the lines-of-sight to pulsars to cut through an HII region? and in some cases more than one HII region* Ideally, the electron density in each HII region must be treated separately from the mean interstellar electron density; but practically we can only deal with this quantity statistically. Under the circumstances a reasonable model for the electron density in the Galaxy would be (Lyne 1981a)

$$n_e(z) = n_{e1} + n_{e2}\, \mathrm{EXP}-(|z|/70) \tag{3.7}$$

where the second term is due to HII regions which are known to have a scale height of $\sim$ 70 pc. In this section we combine a number of different techniques in order to estimate optimum values of n_{e1} and n_{e2}.

(i) Table 3.1 shows 23 pulsars for which reliable independent distances are available (Manchester and Taylor 1981). Thirteen other pulsars for which only distance limits are available have been omitted. For a pulsar at distance d and galactic latitude b_{II} (hence $z = d \sin b_{II}$), eq. (3.7) leads to the following expression for the dispersion measure

$$DM = n_{e1}\, d + n_{e2}\, d' \tag{3.8}$$

where

$$d' = 70\left[1 - \mathrm{EXP}-(|z|/70)\right] / \sin b_{II} \tag{3.9}$$

Here d' is the effective path length through the HII-region zone of the Galaxy, Using data in table 3.1, one can determine

TABLE 3.1

Dispersion measures of pulsars with independently measured distances (taken from Manchester and Taylor (1981)). The iast column shows if the line of sight to the pulsar intersects any known HII region within 1 Kpc from the Sun.

PSR	distance(Kpc)	|z|(pc)	DM(pc.cm^{-3})	HII
0318+59	3.0	110	34.80	no
0329+54	2.3	50	26.78	no
0355+54	1.6	20	57.03	no
0525+21	2.0	240	50.96	no
0531+21	2.0	200	56.79	no
0736-40	2.5	400	160.80	yes
0740-28	1.5	60	73.77	no
0833-45	0.5	20	69.08	yes
0835-41	2.4	10	147.60	yes
1054-62	6.0	310	323.40	yes
1154-62	7.0	20	325.20	yes
1240-64	12.0	320	297.40	yes
1323-62	7.9	30	318.40	no
1356-50	8.8	170	295.00	yes
1557-50	7.8	220	270.00	no
1558-50	2.5	60	169.50	no
1641-45	5.3	20	475.00	yes
1859+03	11.0	120	402.90	no
1900+01	5.0	170	243.40	no
1929+10	0.08	5	3.18	no
2002+31	8.0	0	233.00	no
2111+46	4.3	100	141.50	yes
2319+60	2.8	30	96.00	yes

n_{e1} and n_{e2} by minimising

$$R = \sum_{i=1}^{18} (n_{e1} d_i + n_{e2} d'_i - DM_i)^2 / d'_i \tag{3.10}$$

This leads to n_{e1} =0.0327 cm^{-3}, n_{e2} =0.0138 cm^{-3}. The 1σ permitted region is marked by the curve B in fig. 3.6. Substituting the above values in eq. (3.10) one obtains a value of R which corrsponds to a DM fluctuations of 54.7 pc cm^{-3} per kpc path length, Since the mean DM per kpc is itself only of the order of 35 pc cm^{-3}, this shows that the HII regions, if not treated properly, can completely mask the proportionality between DM and d at short distances*

(ii) For distances within 1 Kpc from the Sun, Prentice and ter-Haar (1969) have developed a scheme to treat the known HII regions individually* We have used their scheme to analyse 217 pulsars with computed distances greater than 1 Kpc (out of 302 pulsars listed by Manchester and Taylor 1977 and Manchester et. al. 1978). Considering the lines of sight of these pulsars only within 1 kpc from the Sun, we find they have a cumulative d' of 136.9 kpc and a cumulative DM of 3225.4 pc cm^{-3} from HII regions* This corresponds to

$$n_{e2} = 0.0236 \ cm^{-3} \tag{3.11}$$

Making liberal allowances for errors, we can safely expect

$$n_{e2} > 0.0236/1.5 = 0.0157 \quad ; \quad n_{e2} < 0.0236 * 1.5 = 0.0353 \tag{3.12}$$

These limits have been plotted as the vertical lines marked C in fig. 3.6. It is significant that the range of n_{e2} in eq. (3.12) is in reasonable agreement with that obtained by the method (i). Also, the fluctuations in DM calculated by the Prentice and

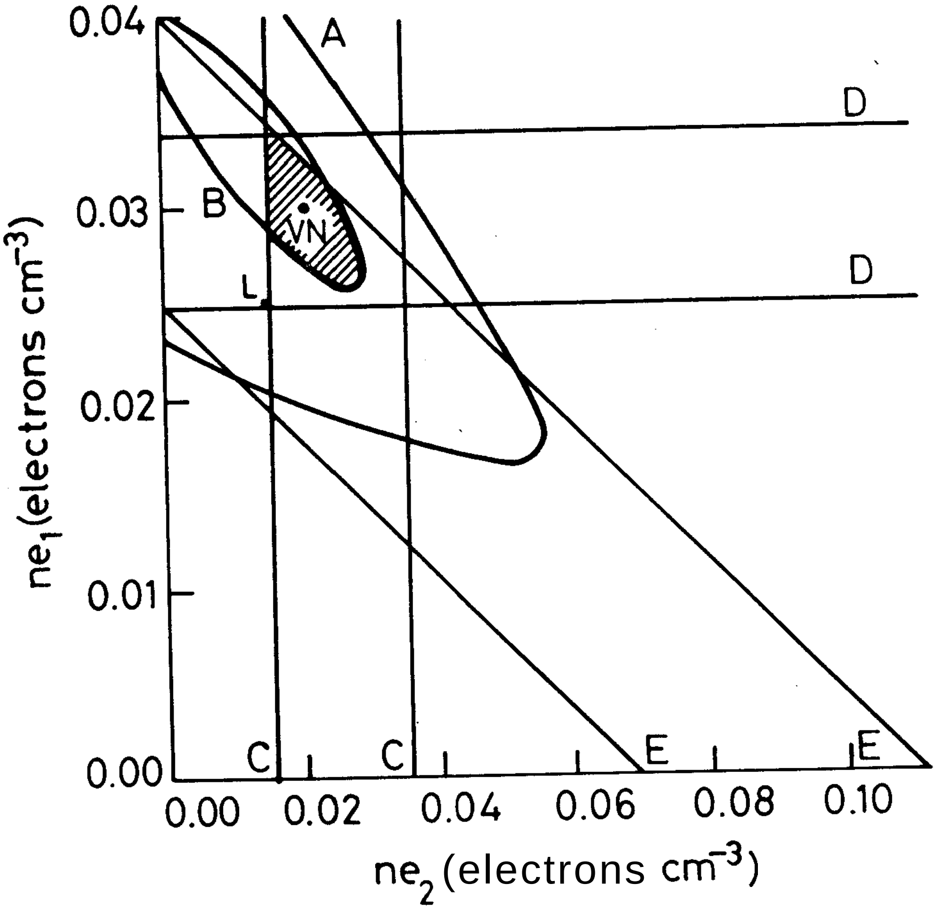

FIG. **3.6** : Optimization of the parameters n_{e1} and n_{e2} in an electron density model of the form eq. (3.7). Curves labelled from A through E show the respective allowed regions in the n_{e1}-n_{e2} space based on five relatively independent arguments:
(a) Cylindrical symmetry of the pulsar distribution in the Galaxy (b) Independent pulsar distances of table (3.1)
(c) Calculation of HII region contribution to the dispersion measures as evaluated by Prentice and ter Haar (1969)
(d) Independent distances of pulsars whose lines of sight do not intersect a known HII region (e) Results of del Romero and Gomez-Gonzalez, 1981. The allowed region common to all the five arguments is shown hatched in the figure. The dot in the centre of this region represents our model (eq. (3.17)). Lyne's (1981a) model is marked L.

ter-Haar formula is 43.3 pc cm^{-3} per kpc path length which agrees with 54.7 estimated by method (i). All these suggest that the Prentice and ter-Haar correction is quite reliable in an average sense, though, in individual cases it might be significantly in error.

(iii) We have tried to approximately estimate n_{e1} as follows. Thirteen pulsars in table 3.1 do not intersect any of the Prentice and ter-Haar HII regions within 1 kpc from the Sun. If we leave out PSR 1323+62 and PSR 2002+31, the cumulative d' of the others, outside the 1 Kpc sphere, is 38.8 Kpc. These numbers suggest that these 11 pulsars mostly sample n_{e1} and interact very little with n_{e2}. We can therefore estimate n_{e1} by means of

$$n_{e1} = \left[\sum_{i=1}^{11} DM_i - n_{e2}\left(\sum_{i=1}^{11} d'_i\right)\right] \Big/ \sum_{i=1}^{11} d_i \tag{3.13}$$

where any reliable value of n_{e2} may be used. Using the limits on n_{e2} given in eq. (3.12) and also allowing for fluctuations in DM due to HII regions, we obtain the following limits on n_{e1}.

$$0.0248\ cm^{-3} < n_{e1} < 0.0337\ cm^{-3} \tag{3.14}$$

These are plotted as the horizontal lines D in fig. 3.6.

3.5 RESULTS

The methods of sections 3.2 and 3.3 can be applied to a model of the type in eq. (3.7) by dividing pulsars into high-z and low-z categories as before and requiring that eq. (3.5) be satisfied* The curve labelled A in fig. 3.6 shows our results* All points within this curve in the $n_{e1} - n_{e2}$ space are allowed, and those outside are unlikely.

del Romero and Gomez-Gonzalez (1981) have estimated that the effective $\langle n_e \rangle$ for regions out to about 5 kpc from the Sun is about 0.03 cm^{-3} By appendix A this implies for the model in eq. (3.7)

$$\langle n_e \rangle = n_{e1} + 0.358\, n_{e2} = 0.03\ cm^{-3} \qquad (3.15)$$

These authors have not given the confidence limits for their estimate of $\langle n_e \rangle$, However, a study of their fig. 2 suggests that the following are very safe bounds

$$0.025\ cm^{-3} < \langle n_e \rangle \ (= n_{e1} + 0.358\, n_{e2}) < 0.040\ cm^{-3} \qquad (3.16)$$

these lines are marked E in fig. 3.6.

Combining these with the results of the previous section we see in fig, 3.6 that the parameters of eq. (3.7) are rather well determined* The hatched region shows the $n_{e1} - n_{e2}$ parameter space that is common to all the different approaches* Our choice for a good model is marked VN in the centre of this regions and corresponds to the following equation

$$n_e(z) = 0.03 + 0.02\ \mathrm{Exp} - (|z|/70) \qquad (3.17)$$

This formula should be used only beyond 1 Kpc from the Sun. Within this sphere we suggest using $\langle n_e \rangle$ =0.03 along with the Prentice and ter-Haar (1969) correction for HII regions*

3.6 DISCUSSION

We have ignored some effects which could possibly affect the validity of our results*

(1) Although it is known that pulsars are found preferably along the spiral arms in the Galaxy (del Romero and Gomez-Conzalez 1981), we have assumed that the pulsar distribution is cylindrically symmetric about the galactic centre* We believe that in an average sense the spiral arm system can be treated as a cylindrically symmetric system* For example, the distribution of pulsar galactocentric longitudes would be essentially uniform, inspite of the spiral structure* Therefore our assumption is unlikely to introduce any, large systematic error in our results*

(2) In our calculations we have treated the HII regions in terms of an equivalent uniform electron density medium. However, the calculations of the previous section show that for small distances ($<$ 2 Kpc) the DM contribution from HII regions can fluctuate consideradly. Thus, at such small distances, the proportionality between DM and d (eq. 3.1) which is fundamental to all our calculations may not be valid* We have been cautious in this matter by deleting from our calculations a volume around the Sun of radius approximately 2 kpc (DM $<$ 60 pc cm^{-3}). However, even at large distances, some fluctuations in $\langle n_e \rangle$ would be present, which we have ignored* Therefore the statistical errors we have quoted may be underestimates*

(3) We have not incorporated any selection effect due to interstellar scattering (ISS) of pulsar radiation* ISS increases with increasing DM ; hence we may miss high DM pulsars* This is believed to be strongest in the inner regions of the Galaxy (say, $|l_{II}| < 30^{\circ}$; Rao, A.P. 1982, personal communication). However since the number of pulsars involved in this volume is small, our results will not be significantly affected*

(4) We have assumed the distance to the galactic centre to he 10 Kpc. If the true distance is, say, 8.7 kpc (Oort 1977), then our electron density values will need scaling by the factor $10/8.7 \sim 1.15$.

None of the above effects is very serious. We therefore believe (from the close agreement of the various independent calculations we have made) that eq. (3.17) models the actual situation rather closely. We do not agree with Arnett and Lerche (1981) who claim that $\langle n_e \rangle$ cannot be known with an accuracy better than a factor of two* We believe that our model is a better approximation than that of Lyne (1981a; marked L in fig. 3.6), which is of course by no means exluded. Pulsar distances computed using our model (eq. 3.17) should be accurate to 20% on the average, though in individual cases the error may be larger.